

7-2018

Epigenetic Alterations Mediate iPSC Normalization of DNA-Repair Expression and TNR Stability in Huntington's Disease

Peter A. Mollica

Martina Zamponi


John Reid

Deepak Sharma

Alyson E. White

See next page for additional authors

Follow this and additional works at: https://digitalcommons.odu.edu/medicaldiagnostics_fac_pubs

 Part of the [Cancer Biology Commons](#), [Diseases Commons](#), [Genetics Commons](#), and the [Translational Medical Research Commons](#)

Authors

Peter A. Mollica, Martina Zamponi, John Reid, Deepak Sharma, Alyson E. White, Roy C. Ogle, Robert D. Bruno, and Patrick C. Sachs

RESEARCH ARTICLE

Epigenetic alterations mediate iPSC-induced normalization of DNA repair gene expression and TNR stability in Huntington's disease cells

Peter A. Mollica^{1,2}, Martina Zamponi^{1,3}, John A. Reid^{1,3}, Deepak K. Sharma¹, Alyson E. White¹, Roy C. Ogle¹, Robert D. Bruno^{1,*} and Patrick C. Sachs^{1,*}‡

ABSTRACT

Huntington's disease (HD) is a rare autosomal dominant neurodegenerative disorder caused by a cytosine-adenine-guanine (CAG) trinucleotide repeat (TNR) expansion within the *HTT* gene. The mechanisms underlying HD-associated cellular dysfunction in pluripotency and neurodevelopment are poorly understood. We had previously identified downregulation of selected DNA repair genes in HD fibroblasts relative to wild-type fibroblasts, as a result of promoter hypermethylation. Here, we tested the hypothesis that hypomethylation during cellular reprogramming to the induced pluripotent stem cell (iPSC) state leads to upregulation of DNA repair genes and stabilization of TNRs in HD cells. We sought to determine how the HD TNR region is affected by global epigenetic changes through cellular reprogramming and early neurodifferentiation. We find that early stage HD-affected neural stem cells (HD-NSCs) contain increased levels of global 5-hydroxymethylation (5-hmC) and normalized DNA repair gene expression. We confirm TNR stability is induced in iPSCs, and maintained in HD-NSCs. We also identify that upregulation of 5-hmC increases ten-eleven translocation 1 and 2 (TET1/2) protein levels, and show their knockdown leads to a corresponding decrease in the expression of select DNA repair genes. We further confirm decreased expression of TET1/2-regulating miR-29 family members in HD-NSCs. Our findings demonstrate that mechanisms associated with pluripotency induction lead to a recovery in the expression of select DNA repair gene and stabilize pathogenic TNRs in HD.

KEY WORDS: Huntington's disease, Ten-eleven translocation, miR-29, Trinucleotide repeat, iPSC

INTRODUCTION

Huntington's disease (HD) is a rare neurodegenerative disorder that is caused by an expansion of cytosine-adenine-guanine (CAG) trinucleotide repeats (TNR) in exon 1 of the *HTT* gene (MacDonald et al., 1993). This pathogenic TNR region is prone to variable

instability in the body, as evidenced by somatic tissue mosaicism and intergenerational differences during disease transmission (Fortune et al., 2000; Langbehn et al., 2004, 2010; Ranen et al., 1995). The mechanisms regulating HD TNR expansions within somatic tissues and germinal cells are not comprehensively understood.

Mutant huntingtin (mHtt) protein has extensive pathogenic effects including transcription factor aggregation, mitochondrial dysfunction, decreased efficacy of DNA damage repair activity and an altered response to oxidative stress (Brustovetsky, 2015; Chang et al., 2012; del Hoyo et al., 2006; Dunah et al., 2002; Glajch and Sadri-Vakili, 2015; Jonson et al., 2013; Mann et al., 1990; McQuade et al., 2014; Nucifora et al., 2001; Tsoi et al., 2012; Zhai et al., 2005). Furthermore, recent evidence from our laboratory and others demonstrates that the presence of mHtt also affects various epigenetic mechanisms (Buckley et al., 2010; Mollica et al., 2016; Suzuki and Bird, 2008). Specifically, we previously reported that DNA methylation in HD patient-derived fibroblasts leads to downregulation of a subset of DNA repair genes and TNR instability (Mollica et al., 2016). These selected DNA repair genes, *APEX1*, *BRCAL*, *RPA1* and *RPA3*, are known effectors of TNR stability (Andreoni et al., 2010; Beaver et al., 2015; Broderick et al., 2010; Crespan et al., 2015; Li et al., 2014; Mason et al., 2014; Spiro and McMurray, 2003). Furthermore, we also demonstrated that inducing hypomethylation with a DNA methyltransferase inhibitor resulted in TNR stabilization. These data identify potential epigenetic involvement in HD that controls TNR stability and genomic integrity. Furthermore, these data have potentially important implications for mechanisms of genetic anticipation, disease development and possible therapeutic treatments. However, the application of these findings to developmental models and disease relevant cells is of obvious interest.

Induced pluripotent stem cell (iPSC) technology is attractive, not only for novel therapies, but also for generation of HD and other neurodegenerative experimental models where access to disease-specific cell types is not feasible (Choi et al., 2014; Hick et al., 2013; Kaye and Finkbeiner, 2013; Lee and Huang, 2017; Nayler et al., 2017; Nenasheva et al., 2016). One of the most recognized characteristics of iPSCs is the global epigenetic changes involved in reprogramming, as multiple studies have identified extensive differential regulation of epigenetic elements and patterns (Carey et al., 2011; Hewitt et al., 2011; Leung et al., 2014; Vaskova et al., 2013). Of these epigenetic mechanisms, microRNAs such as miR-29 family members have been shown to affect active demethylation mechanisms in iPSCs due to their regulatory interactions with members of the ten-eleven translocation (TET) protein family (Morita et al., 2013; Zhang et al., 2013). The TET family proteins actively catalyze the conversion of 5-methylcytosine (5-mC)

¹Department of Medical Diagnostic and Translational Sciences, Old Dominion University, Norfolk, VA 23529, USA. ²Molecular Diagnostics Laboratory, Sentara Norfolk General Hospital, Norfolk, VA 23507, USA. ³Biomedical Engineering Institute, Old Dominion University, Norfolk, VA 23529, USA.

*These authors contributed equally to this work

‡Authors for correspondence (psachs@odu.edu; rbruno@odu.edu)

© P.A.M., 0000-0002-0621-2819; M.Z., 0000-0002-9154-1667; J.A.R., 0000-0003-2989-1292; D.K.S., 0000-0003-2844-8790; A.E.W., 0000-0001-7222-0916; R.C.O., 0000-0002-4231-9488; R.D.B., 0000-0003-3329-9478; P.C.S., 0000-0002-0871-6789

into 5-hydroxymethylcytosine (5-hmC), restructuring the DNA methylation-based epigenetic landscape during the process of acquiring pluripotency (Dawlaty et al., 2014; Hysolli et al., 2016; Ito et al., 2010). Interestingly, miR-29 has also been reported to be differentially expressed in primary HD cells in microRNA expression screens (Johnson et al., 2008; Martí et al., 2010). Furthermore, TET proteins, 5-mC and 5-hmC have emerged as being involved in neurodegenerative diseases, such as Parkinson's disease, Alzheimer's disease, amyotrophic lateral sclerosis, as well as in HD (Al-Mahdawi et al., 2014; Buckley et al., 2010; Pan et al., 2016; Rudenko et al., 2013; Santiago et al., 2014).

With this data taken together, we set out to investigate the effects that epigenetic reconstruction, via reprogramming HD affected fibroblasts to a pluripotent state and subsequent neural stem cell (NSC) differentiation, would have on DNA repair gene expression and TNR instability. We determine that, during reprogramming, 5-hmC levels are increased similarly in both wild-type and HD iPSCs, but that 5-hmC remains significantly elevated in HD cells during differentiation to neuronal stem cells. This increase correlated with an increase in DNA repair gene expression and TNR stability, consistent with our previous results. Finally, we demonstrate that the increase in 5-hmC levels is likely due to an increase in TET protein expression, mediated by decreased expression of miR-29a/b in HD-NSCs. These data have important implications for our understanding of disease progression, and the mechanisms of TNR instability in HD.

RESULTS

HD iPSCs and NSCs show increased DNA repair gene expression

We previously identified downregulated gene expression of the DNA repair genes *APEX1*, *BRCA1*, *RPA1* and *RPA3* in multiple HD fibroblast cell lines derived from patients, and that their expression could be recovered upon forced hypomethylation (Mollica et al., 2016). Owing to the global epigenetic restructuring that occurs during iPSC reprogramming, we sought to determine how those epigenetic changes would affect DNA repair gene expression in HD cells. To accomplish this, wild-type (Wt) and HD-affected cell lines were reprogrammed to iPSCs (Fig. S1) and then differentiated into NSCs (Fig. S2). At population doubling (PD) 10 of each cell state (iPSC and NSC), total RNA was collected to determine the gene expression of *APEX1*, *BRCA1*, *RPA1* and *RPA3*. Relative to their expression at the pre-reprogrammed fibroblast state, both HD-iPSCs and HD-NSCs showed increased expression of all repair genes analyzed, while expression in Wt cells remained constant (Fig. 1). Furthermore, no significant differences in expression were observed for any of the genes in HD-iPSCs or HD-NSCs relative to WT-iPSCs and WT-NSCs, respectively. Therefore, the reprogramming process rescues the expression of DNA repair genes *APEX1*, *BRCA1*, *RPA1* and *RPA3* in HD cells, and the rescued phenotype persists through NSC differentiation.

TNR regions of *HTT* gene remain stable after pluripotency induction and during early-stage neuronal differentiation

With the witnessed normalization of DNA repair gene expression in HD-affected iPSCs and NSCs, we next wanted to determine how changes in differentiation status affected the pathogenic repeat expansion in the *HTT* gene. Genomic DNA samples were collected from the HD1 fibroblast line at PD 12 and 20, and HD2 fibroblast line at PD 8 and 16, as well as from iPSC-HD1, iPSC-HD2 cells, and HD1-NSCs and HD2-NSCs at PD 0 and PD 20 for TNR expansion analysis. By performing capillary electrophoresis-based

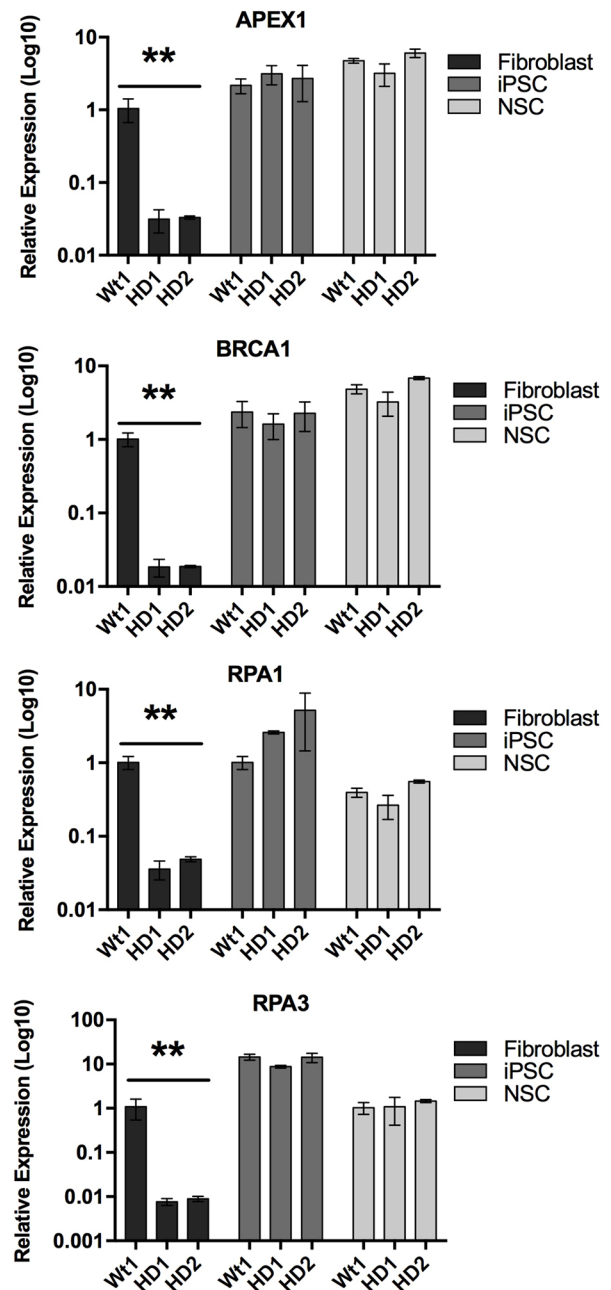


Fig. 1. HD-iPSCs and -NSCs show recovery of expression of select DNA repair genes to Wt levels. qRT-PCR for *APEX1*, *BRCA1*, *RPA1* and *RPA3* mRNA levels through NSC differentiation. Gene expression for all DNA repair genes was downregulated in HD fibroblasts relative to those in Wt. During reprogramming and after NSC differentiation all repair genes were upregulated to Wt levels. Fold change is relative to the average mean expression of two native wild-type cell lines. Results are mean \pm s.d. for each replicate. All experiments were conducted in triplicate and compared by a one-way ANOVA with Dunnett's post hoc (** $P < 0.01$).

fragment analysis, it was revealed that HD1 fibroblasts contained 18/43 CAG repeats at PD 12 and 18/44 CAG repeats at PD 20. HD2 fibroblasts contained 17/41 CAG repeats at PD 8 and 17/42 at PD 16, within the *HTT* gene (Fig. 2A,B; Fig. S3C,D). HD1 and HD2 continued to maintain the same size TNR region immediately following iPSC reprogramming, and throughout 20 PDs post-reprogramming with repeats of 18/44 and 17/42, respectively (Fig. 2A,B; Fig. S3A,B). Fragment analysis of HD1-NSC and HD2-

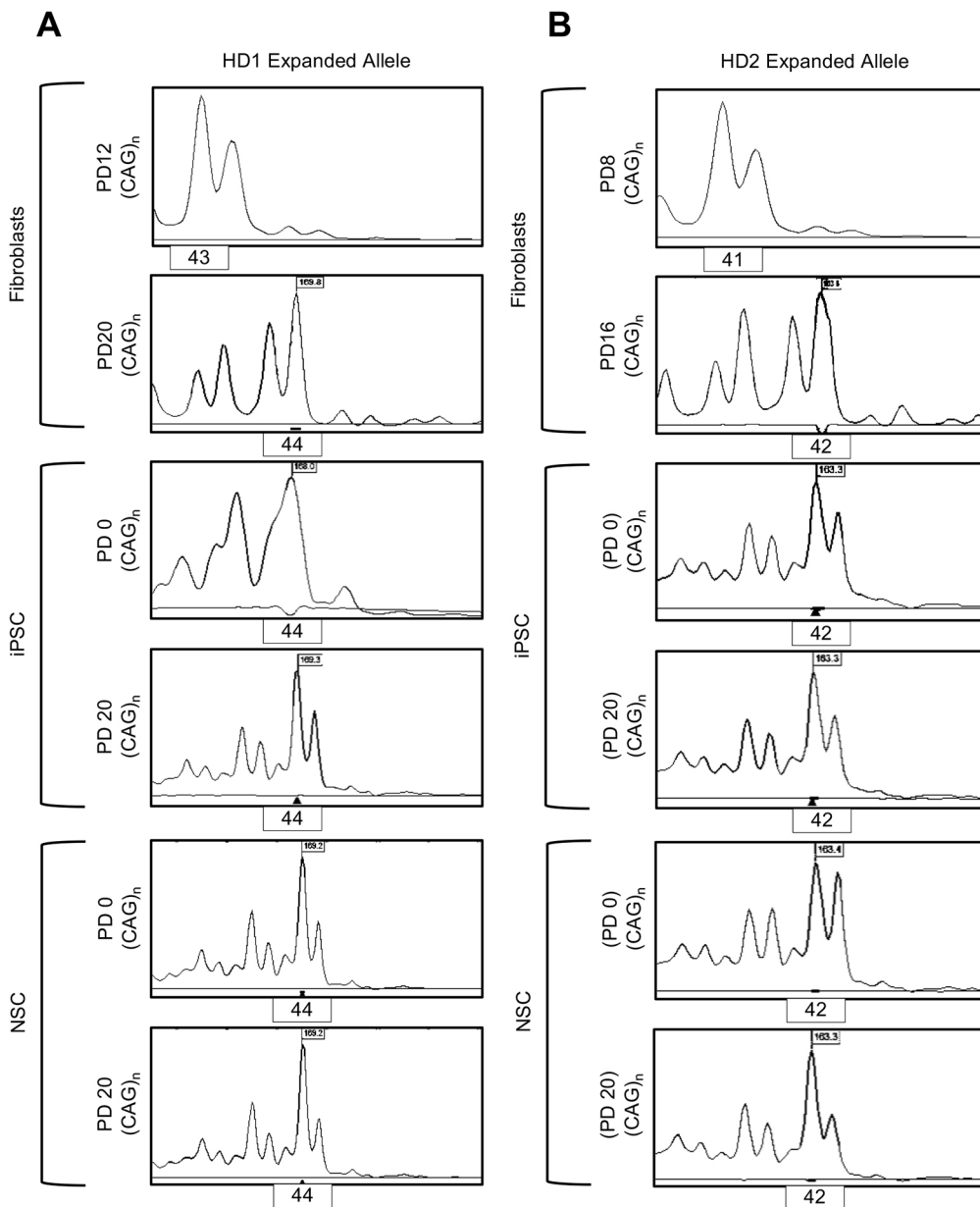


Fig. 2. HD-affected iPSC and NSCs show trinucleotide repeat stability through 20 PDs. (A) Fragment analysis of gDNA samples extracted from patient-derived HD fibroblast sample HD1 shows that the *HTT* pathogenic allele containing 43 CAG trinucleotide repeats at PD 12 and then 44 CAG repeats immediately prior to reprogramming (row 1). Analysis of successfully reprogrammed HD1-iPSC samples show that the 44 CAG repeats are maintained from PD 0 (row 2) to PD 20 (row 3). Immediately after NSC differentiation (row 4), and 20 PD later (row 5), gDNA fragment analysis shows 44 CAG repeats. (B) TNR analysis of HD2 fibroblasts at PD 8 shows that there are 41 CAG repeats and then 42 CAG repeats at PD 20, prior to reprogramming (row 1). Immediately following iPSC reprogramming (row 2) and 20 population doublings later (row 3), the number of CAG repeats remain at 42. Following NSC differentiation (row 4) and successive passaging for 20 PDs (row 5), the TNR region shows stability with 42 CAG repeats.

NSCs genomic (g)DNA at PD 0 and 20 also revealed no change had occurred in the number of CAG repeats from their iPSC state (Fig. 2A,B). These data on TNR region stability from iPSC reprogramming to neural induction are in direct contrast to our published findings in the HD fibroblast lines, which demonstrate a rapid expansion within 8 PDs (Mollica et al., 2016). Thus, we conclude that inherent features of the reprogramming process result in the stabilization of the pathological TNR repeat region within the *HTT* gene. Interestingly, upon successful neural induction into NSCs, both HD cell lines maintained the initial CAG repeat lengths originally seen in their fibroblast state, indicating a retained TNR stabilization (Fig. 2).

HD-affected NSCs have increased global 5-hmC

The epigenetic landscape has been shown to shift dramatically during iPSC reprogramming. One of the novel epigenetic mechanisms reportedly involved in reprogramming is the increased presence of 5-hydroxymethylcytosine (5-hmC)

production. As we witnessed an increase in select DNA repair gene expression, which coincided with TNR stability, we hypothesized that epigenetic mechanisms related to gene activation had occurred during reprogramming and were maintained during differentiation. More so, following reports of differential presence of 5-hmC in HD cells, we identified this as a possible mechanism for our observed results (Glajch and Sadri-Vakili, 2015; Lee et al., 2013; Wang et al., 2013). We analyzed gDNA samples extracted from all diseased and unaffected fibroblasts, iPSCs and NSCs (collected at PD 20) to determine the global percentages of 5-hmC presence through sandwich-based ELISA (Fig. 3A). We found that the pre-reprogrammed HD fibroblasts did not show significant differences in the percentage of global 5-hmC in comparison to the pre-reprogrammed Wt fibroblast cells. In addition, there was no significant difference in the percentage 5-hmC presence after induction of pluripotency of diseased versus unaffected cells. However, we did witness substantial increases in 5-hmC presence in all iPSCs when compared

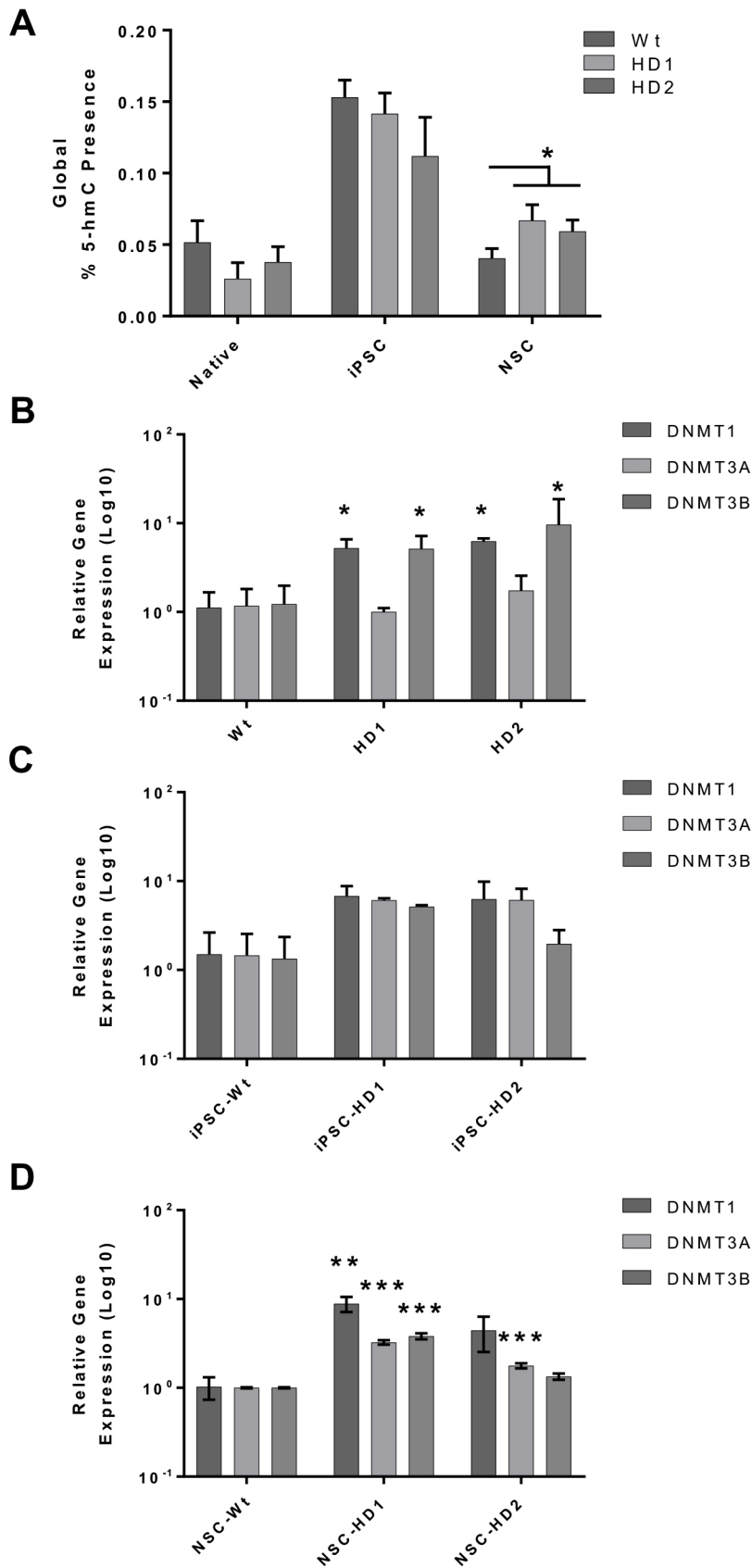


Fig. 3. Altered 5-hmC and DNMT protein expression in HD-NSCs. (A) Global 5-hmC levels were analyzed for each cell type/state. HD1 and HD2 had statistically significant increases in 5-hmC levels as compared to Wt controls. Results are mean \pm s.d. for the percentage of 5-hmC between each of the six gDNA samples. (B) qRT-PCR analysis of *DNMT1*, *DNMT3A* and *DNMT3B* revealed significantly greater levels of *DNMT1* and *DNMT3B* mRNA levels in HD1 and HD2 fibroblasts as compared to Wt controls. (C) When reprogrammed into iPSCs, HD1 and HD2 cells had no significant differences in DNMT mRNA levels compared to controls. (D) Upon differentiation to NSCs, significant differences in DNMT expression were again observed in HD cells compared to Wt controls. Results are the mean \pm s.d. fold regulation of each sample. All experiments were conducted in triplicate and compared with a one-way ANOVA with Dunnett's post hoc (* P <0.05, ** P <0.01, *** P <0.001).

to their fibroblast state, verifying that methylation patterning undergoes extensive changes during cellular reprogramming. Interestingly, the percentage levels of global 5-hmC presence in NSC-HD1 and

NSC-HD2 were significantly increased relative to the control NSCs. gDNA samples from NSC-HD1 and NSC-HD2 cells contained 0.066% and 0.059% 5-hmC residues, respectively, relative to the

mean of the Wt samples, which contained 0.040% (Fig. 3A). These data reveal that the epigenetic landscape is altered during neurodevelopment in response to the presence of mHtt.

Differential expression of DNMT proteins in HD-affected iPSCs and NSCs

We had previously reported HD-specific differential methylation patterns in the promoter regions of the DNA repair genes (Mollica et al., 2016). While the increased presence of 5-hmC in HD-NSCs is indicative of active demethylation, we next sought to characterize the status of active methylation across each cell state. Here, we evaluated gene expression of *DNMT1*, *DNMT3A* and *DNMT3B*, for which the encoded proteins are involved in active methylation of newly synthesized DNA. In the native, fibroblast cell state, both *DNMT1* and *DNMT3B* showed statistically significant upregulation in both HD samples as compared to Wt (Fig. 3B), consistent with increased methylation at select promoter sites, as we have previously shown (Mollica et al., 2016). Expression analysis of Wt- and HD-iPSCs revealed no statistical difference in expression between the groups, indicating that, during reprogramming, the levels of these genes return to normal (Fig. 3C). Furthermore, analysis of DNMT genes in all NSC lines showed that gene expression of *DNMT3A* was slightly upregulated in both HD samples (Fig. 3D). Furthermore, NSC-HD1 cells showed increased expression of *DNMT1* and *DNMT3B*. These data suggest that during pluripotency induction, the expression of factors involved in active DNA methylation is corrected in HD cells. However, although HD-NSCs begin to exhibit dysregulation of components involved in epigenetic regulation, this data reveals that dysregulation is occurring in different components (*DNMT3A*), while the native HD fibroblasts showed no dysregulation in *DNMT3A*. This upregulation of *DNMT3A* may be counterbalanced, however, by an increase in active demethylation as indicated by the increased levels of 5-hmC shown above (Fig. 3A).

Dysregulated TET1/2 expression in HD-affected neural stem cells

Recently, studies have demonstrated that 5-mC can be actively converted into 5-hmC by the ten-eleven translocation (TET) family proteins (Zhang et al., 2013). Moreover, evidence is mounting for the critical involvement of TET proteins in maintaining enriched levels of 5-hmC in iPSCs and neural cell types (Ito et al., 2010; Koh et al., 2011; Kriaucionis and Heintz, 2009). Thus, we next wanted to confirm whether the increased 5-hmC presence in HD-NSC lines was due to alterations of TET family proteins. We conducted gene expression analysis of pre-reprogrammed fibroblasts, iPSC and NSC cell types from unaffected and HD patients for *TET1* and *TET2*. HD-affected fibroblasts and iPSCs, showed no *TET1* or *TET2* gene dysregulation when compared to expression levels in Wt controls (Fig. 4A, left and middle). However, NSC-HD1 and NSC-HD2 lines showed significant increases in *TET1* expression, with NSC-HD1 also having significant upregulation of *TET2* (Fig. 4A, right). By determining the relative fluorescence intensity in immunocytochemistry experiments, we evaluated the relative presence of both proteins using dual-staining methods (Fig. 4B). Fluorescence intensity calculations showed increased protein expression of *TET1* in both HD-NSC samples (Fig. 4C, top) and increased protein expression of *TET2* in NSC-HD1 (Fig. 4C bottom), normalized to unaffected NSC samples. Differences in *TET1* and *TET2* protein expression were further confirmed in western blotting and spot densitometry experiments (Fig. 4D). This corroborates our immunocytochemistry analysis, authenticating

TET1 upregulation in NSCs affected by HD. To verify a link between *TET* expression and expression of select DNA repair genes, we evaluated the expression of *APEX1*, *BRCA1*, *RPA1* and *RPA3* on NSC-HD2 cells when siRNA targeting *TET1* and *TET2* were introduced. Introduction of siRNA targeting *TET1* and *TET2* led to decreased expression of endogenous levels of available *TET1* and *TET2* mRNA (Fig. 5A). Furthermore, gene expression analysis revealed significantly decreased levels of *RPA1* in response to siRNA targeting *TET2*, and *APEX1* and *RPA3* when cells were treated with both siRNA targeting *TET1* and *TET2* (Fig. 5B). This data supports a link between *APEX1* and *RPA1* expression and *TET1/2* levels in HD-affected neural stem cells. Furthermore, these data together explain the relative increased levels of 5-hmC presence seen in HD-affected NSCs, and is consistent with the interpretation that upregulation in components of methylation pathways are a proportional response to mobilized active demethylation.

HD-affected NSCs exhibit decreased expression of miR-29a/b

Since the verification of TET family proteins, and mechanisms with the capability to actively demethylate DNA, there has been extensive investigation into its regulation, especially concerning its involvement in mammalian development, cancer and stem cell self-renewal (Dawlaty et al., 2014; Ito et al., 2010; Kinney and Pradhan, 2013). One of the most recognized regulators of *TET1/2* is the microRNA pathway, specifically the miR-29 miRNA family (miR-29a, miR-29b and miR-29c) (Morita et al., 2013). Importantly, there have been previous reports that miR-29 family members are dysregulated in HD, including in HD neuronal cell types (Johnson et al., 2008; Martí et al., 2010). As this presents a clear explanation of the changes we were witnessing, here we wanted to see whether miR-29 dysregulation was related to the upregulation of *TET* in HD. Quantitative (q)PCR of HD-affected fibroblasts confirmed previous findings of dysregulation in the members of the miR-29 family, relative to wild-type levels (Fig. 5C). However, expression of miR-29a, -29b and -29c was not changed in HD-iPSCs when compared to the levels in Wt iPSCs (Fig. 5D). Strikingly, HD-NSCs showed significant decreases in expression of miR-29a and miR-29b (Fig. 5E). These data, taken together, identify the miR-29 epigenetic regulatory pathway as being affected by early-stage HD during neurodevelopment. Moreover, this expression of miR-29 members in HD fibroblasts and HD NSCs fits the expression pattern of *TET* proteins, thereby providing a possible mechanism for the increased 5-hmC presence witnessed in HD-NSCs.

DISCUSSION

Although it is clear that TNR expansions within the *HTT* gene are a hallmark of HD, it remains unclear why unregulated expansions occur throughout the lifespan of HD patients, but do not occur during embryonic development (Kovtun et al., 2004; Mangiarini et al., 1997). As TNR expansions are associated with the age of onset and severity of the disease, comprehensive understanding of the process could lead to therapeutic interventions aimed at stabilizing TNR regions, delaying the onset of the disease and minimizing genetic anticipation in subsequent generations.

While the comprehensive mechanism of pathological HD TNR instability is poorly understood, it is agreed that endogenous DNA repair mechanisms are involved. We previously identified *APEX1*, *BRCA1*, *RPA1* and *RPA3* as being consistently downregulated across multiple HD lines, and demonstrated that their

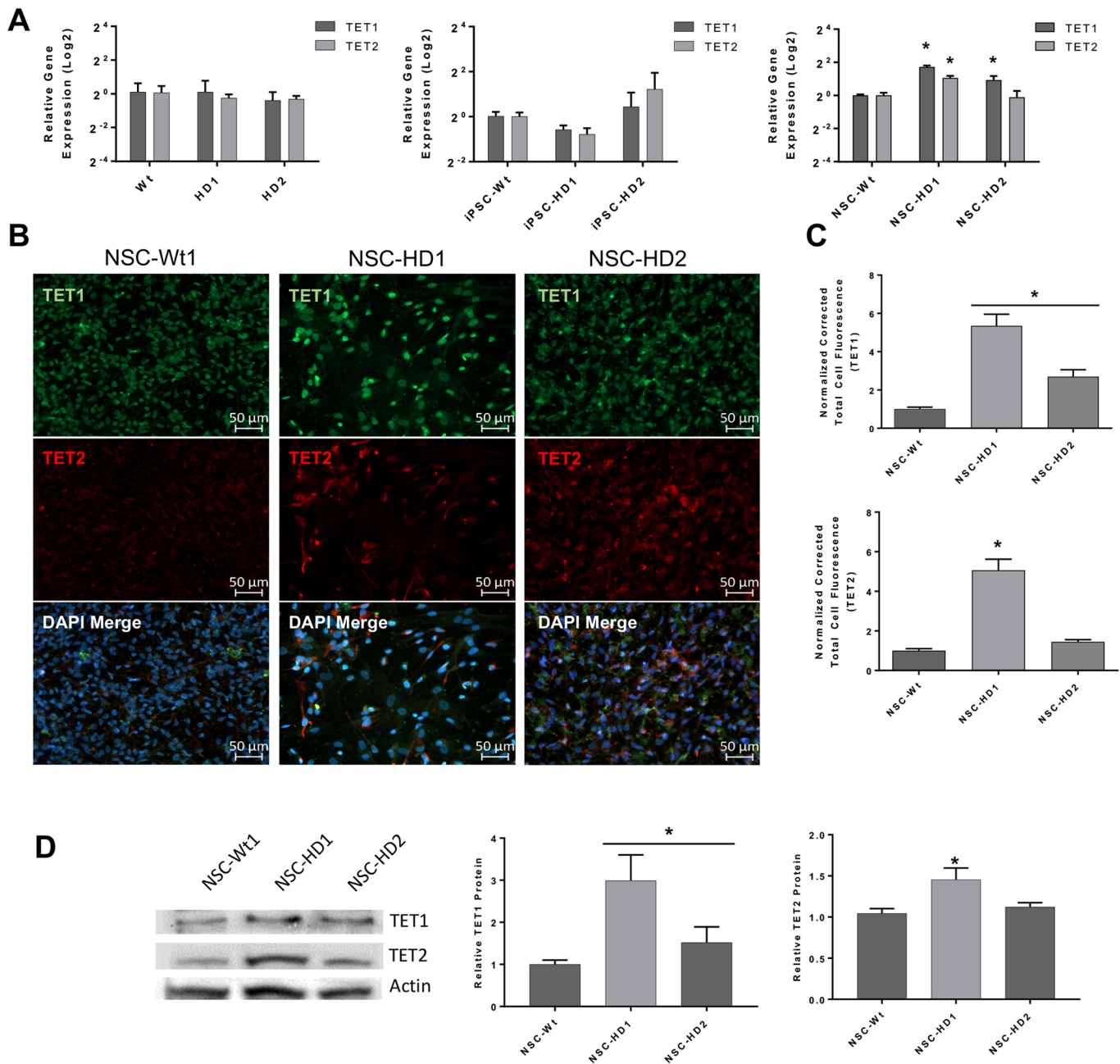


Fig. 4. HD-affected neural stem cells show upregulated TET protein expression. (A) Gene expression analysis of *TET1* and *TET2* in HD and Wt fibroblasts (left), HD and Wt iPSCs (middle), and HD and Wt NSCs (right) reveal that there is a statistically significant upregulation of *TET1* and *TET2* in the NSC state. (B) Immunofluorescence staining confirmed the increase in TET1 and TET2 in HD-NSCs. TET1 protein expression (top panels) shown in green and TET2 protein expression (middle panels) shown in red. All cells were counterstained with DAPI (bottom panels). (C) Quantification of fluorescent images shown in B. (D) Western blot and spot densitometry quantification of NSC samples also confirmed upregulation of TET1 and TET2. Results are the mean \pm s.d. for each replicate. All experiments were conducted in triplicate and compared with a one-way ANOVA with Tukey post-hoc ($*P < 0.05$).

downregulation was epigenetically mediated (Mollica et al., 2016). These genes have also previously been identified as effectors of TNR instability (Andreoni et al., 2010; Beaver et al., 2015; Li et al., 2014; Mason et al., 2014). APEX1 in particular has been shown to be required for the maintenance of TNRs (Beaver et al., 2015). Furthermore, all three of these genes are involved in base excision repair, highlighting the potential for a collective aberrant effect on genome instability, as witnessed in other trinucleotide repeat diseases (Goula and Merienne, 2013; Liu and Wilson, 2012). In addition, it should be noted that as TNR stability/instability is a

function of DNA repair, and therefore when measured with TP-PCR and capillary electrophoresis, can act as a surrogate marker of repair processes (Dion, 2014; Dragileva et al., 2009; Goula et al., 2009; Zhao and Usdin, 2015). Therefore, the rescue of expression of this subset of DNA repair genes through cellular reprogramming is significant, and consistent with our previous findings that hypomethylation leads to stabilization of TNRs (Mollica et al., 2016).

Here we propose a model in which mHtt interferes with normal epigenetic regulation, leading to downregulation of key DNA repair

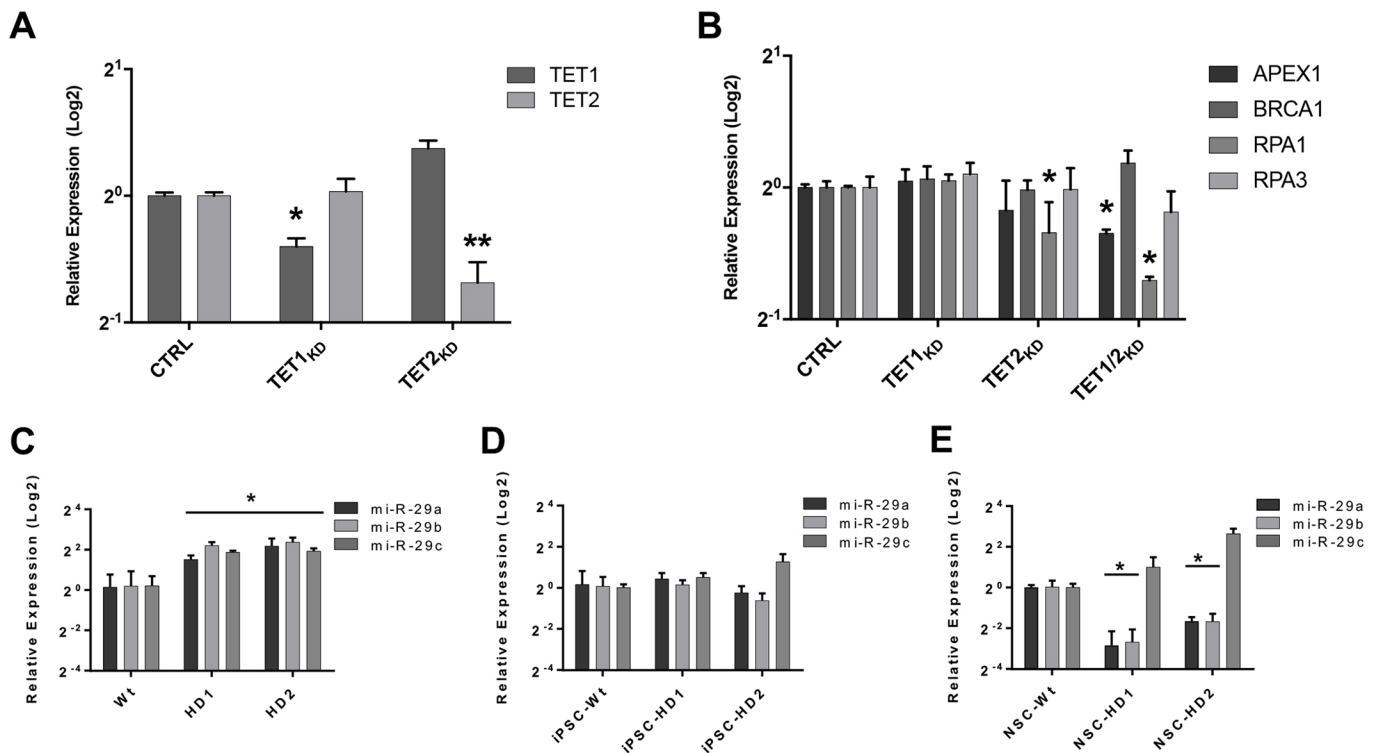


Fig. 5. TET knockdown decreases expression of select DNA repair genes, and TET-regulating miR-29a/b/c are differentially expressed in HD fibroblasts and HD-NSCs. (A) qRT-PCR confirmation of siRNA-targeted knockdown of *TET1* and *TET2* mRNA in HD fibroblasts. (B) The DNA repair genes *APEX1*, *RPA1* and *RPA3* show downregulation in response to combined partial knockdowns of *TET1* and *TET2* in NSC-HD2 cells. (C) Expression analysis demonstrating significantly increased expression of miR-29a/b/c in HD fibroblasts compared to controls. (D) No significant differences in miR-29a/b/c levels were seen in HD-iPSC lines. (E) HD-NSCs expressed significantly less miR-29a/b than Wt controls. Results are the mean \pm s.d. for each replicate. All experiments were conducted in triplicate and compared with a one-way ANOVA with Dunnett's post hoc (* P <0.05; ** P <0.01).

proteins, which, in turn, promotes TNR expansions. Our previous data identified a potential link between methylation, expression of select DNA repair genes and TNR stability in HD patient-derived fibroblasts (Mollica et al., 2016). With the data presented here, we show that mechanisms involved in pluripotency reprogramming correct these previously reported deficiencies in DNA repair genes, corresponding with an increase in TNR stabilization. The stabilization of the iPSC TNR regions might be mediated by the global shifts in DNA methylation patterns seen during reprogramming, mimicking our findings in HD fibroblasts treated with a DNMT inhibitor (Mollica et al., 2016). We were surprised to find no differences in DNA repair gene expression between Wt and HD cells following NSC induction; however, consistent with our model, TNR regions of HD-affected NSCs remained stable.

Genome-wide loss of 5-hmC in HD, and a resultant hypermethylation has been previously reported and extensively implicated in dysfunctional neurogenesis, neuronal function and survival (Al-Mahdawi et al., 2014; Wang et al., 2013). However, our findings demonstrate that 5-hmC levels were either normal or increased in HD cells following reprogramming. In addition, we show that both DNMT1 and DNMT3B are upregulated in the HD fibroblast cells and HD-NSCs. This suggests that DNMT expression seems to be balanced by an increase in 5-hmC and TET levels in HD-iPSC and HD-NSCs. This supports the notion that the pluripotent state has a protective effect on HD-derived neuronal cells. Other findings bolster this claim, such as the finding that transplanted human HD-iPSC into the striatum of mice show delayed HD phenotypes, indicating mechanisms altered in reprogramming affect symptom presentation (Jeon et al., 2014).

This suggests that the increased active demethylation processes help maintain normalized DNA repair gene expression and TNR stability. While the decline of HD-iPSC-derived cells would be expected to start upon differentiation, ultimately leading to a loss in DNA repair gene expression and TNR stability, it is possible that years of expression of the mHtt protein is required for cumulative epigenetic effects to occur following iPSC reprogramming. Finally, we also implicate miRNA-29 dysregulation as a possible mechanistic link resulting in the epigenetic shifts seen during the iPSC to NSC transition. miR-29 targets *TET1* and has been previously indicated as a possible regulatory protein in HD (Johnson et al., 2008; Morita et al., 2013; Roshan et al., 2014). Furthermore, through partial knockdown of *TET1* and *TET2*, we show that these proteins have a direct link to DNA repair gene expression of *APEX1* and *RPA3*, necessary components of the base excision repair pathway, which has been implicated as an effector of TNR instability. We also recognize that the observed increase in 5-hmC presence may either be directly related to mHtt interactions, and, therefore, deleterious over time, or may be a protective countermeasure in response to increased methylation (5-mC) accumulation (Ng et al., 2013). While this remains speculation, it is a critical area in need of future study.

In the short time iPSC reprogramming has been available, research using HD-iPSCs has recognized that pluripotent cells affected by HD show differentially expressed proteins and also that HD-iPSC models maintain the disease phenotype after differentiation and transplantation. These data support our findings that TNR regions are stabilized during pluripotency and early differentiation (Chae et al., 2012; HD iPSC Consortium, 2012;

Jeon et al., 2014, 2012; Juopperi et al., 2012). These data also give some indication that the *in vitro* methods we employed to study these TNR dynamics have some translatable effect. These data combined provide insight into the mechanism behind adult somatic instability, and the resulting genetic anticipation. Furthermore, our data demonstrate a possible mechanism of pluripotency-induced normalization of cellular function and TNR stability and the subsequent contraction bias witnessed in embryonic development.

MATERIALS AND METHODS

Cell lines and culture

Two previously confirmed HD fibroblast cell lines (GM02191 and GM04022) were purchased from Coriell Cell Repositories (Camden, NJ) at early passages (3 and 4, respectively). Two Wt breast-derived adipose stem cells (bASC3 and bASC8) were previously isolated (Sachs et al., 2012; Zhao et al., 2012). HD fibroblast and bASC lines were cultured in Dulbecco's modified Eagle's medium (DMEM) containing Glutamax (Gibco, Gaithersburg, MD), supplemented with 10% premium fetal bovine serum (Life Technologies) and 1% antibiotic-antimycotic (100×) (ABAM; Life Technologies). Medium was replenished between 72 and 96 h after seeding. Cells were cultured in a T-75 flask and passaged upon reaching 75–85% confluency using TrypLE Express (Gibco) following the manufacturer's protocol. Cell lines were maintained at 37°C in a humidified incubator with 5.0% CO₂. For simplicity, in the rest of the paper, GM04022 is denoted HD1, GM02191 is denoted HD2, bASC3 is denoted Wt1, and bASC8 is denoted Wt2.

iPSC reprogramming

To generate stable pluripotent cells, on day 0, 2.5×10^5 – 3×10^5 cells were infected using Sendai viral vectors expressing KOS (Klf4, Oct3/4 and Sox2), c-Myc, and Klf4 using the CytoTune™ –iPS 2.0 Sendai Reprogramming kit (Life Technologies, Carlsbad, CA). Cells were transformed according to the manufacturer's protocol, and lot specification (Lot# L2120009) of Sendai viral components, using a multiplicity of infection (MOI) of 5:5:3. On day 7 post transduction, cells were plated onto irradiated murine embryonic fibroblasts (iMEFs) (Globalstem; Gaithersburg, MD). After confirmation of TRA-1-81-positive pluripotent cells (with antibody from Stemgent®; Lexington, MA), colonies were manually split and passaged for expansion. Upon initial expansion, all iPSC lines were adapted to a feeder-independent protocol using plates coated with Geltrex® LDEV-free reduced growth factor basement membrane Matrix (Life Technologies, Carlsbad, CA) at a concentration of 140–150 µg/ml and were continuously cultured in mTeSR™1 (Stemcell™ Technologies, Vancouver, Canada) for the remainder of our experiments. iPSC lines adapted to mTeSR were passaged and split at ratios of 1:6 to 1:9 using 1 U/ml dispase (Stemcell™ Technologies). Media was replenished on all pluripotent cell lines every 24 h.

After pluripotent transformed colonies were observed, a live-cell pluripotency stem cell marker, anti-TRA-1-81 antibody conjugated to Alexa Fluor 488 (1:200, Stemgent, Lexington, MA), was added to cultures and allowed to incubate for 30 min at 37°C, to identify pluripotent-positive colonies. After live-stain confirmation, TRA-1-81-positive colonies were manually picked off and plated onto murine embryonic fibroblasts after 28 days. Following expansion of TRA-1-81 colonies, alkaline phosphatase (AP) expression was detected by using alkaline phosphatase kit II (Stemgent®, Lexington, MA) according to the recommended protocol. Furthermore, subsets of each pluripotent cell line were analyzed for gene expression of pluripotency markers using qPCR (see section on gene expression below) and a teratoma assay (as described below).

Teratoma assay

The tri-lineage differentiation potential of iPSCs were determined by a modified teratoma assay. iPSC colonies were manually excised from culture dishes and injected into the epithelial divested mammary fat-pads of 3-week-old female Nu/Nu mice (Charles River Laboratories) using surgical procedures previously described (Boulanger et al., 2013, 2012; Bruno et al.,

2014, 2017; Bussard et al., 2010; Zhao et al., 2012). Teratomas were excised 8 weeks post injection, fixed in 10% neutral-buffered formalin (NBF) for 24 h, and then paraffin embedded for immunohistological characterization with H&E. All mice were housed in an Association for Assessment and Accreditation Laboratory Animal Care (AALAC)-accredited facility. All procedures were approved by the Old Dominion University Institutional Animal Care and Use Committee (IACUC).

NSC induction and characterization

iPSCs underwent NSC induction using STEMdiff Neural Induction Medium (NIM) (Stemcell™ Technologies) and AggreWell™ 800 (Stemcell™ Technologies) according to the manufacturer's protocol. Briefly, 3.0×10^6 cells were put into single-cell suspension using dispase, washed with NIM, and plated into a single well of the AggreWell™ 800 plate with NIM supplemented with 10 µM Y-27632 (Sigma Aldrich, St Louis, MO). Cells were centrifuged at 100 g for 3 min and then incubated at 37°C in a humidified incubator containing 5.0% CO₂. Partial medium changes were conducted daily for 4 days. On day 5, embryoid bodies were removed and filtered through a 40-µm strainer and plated onto a Geltrex®-coated six-well plate in NIM. Daily medium changes were conducted from days 6–11. On day 12, neural rosettes were gently dislodged using STEMdiff™ Neural Rosette Selection Reagent (Stemcell™ Technologies) and expanded on Geltrex-coated dishes. Full medium changes occurred for the remainder of the 19-day differentiation. Following characterization (see section on confirmation of neural stem cell differentiation below), NSCs were maintained in StemPro® NSC SFM medium supplemented with 10 ng/ml bFGF, 10 ng/ml EGF, and 1× ABAM, and medium was replenished every other day.

Following neural stem cell differentiation, 5.0×10^4 cells were plated onto Geltrex-coated slides (1:50) and allowed to attach for 48 h. Cells were fixed with 10% NBF for 1 h, permeabilized with 100% ice-cold methanol for 15 min at –20°C, and blocked with 10% goat serum in Tris-buffered saline at room temperature for 1 h. Samples were probed with antibodies for nestin (10C2, 1:100, Thermo Fisher Scientific), PAX6 (13B10-1A10, 1:200, Thermo Fisher Scientific), SOX1 (ab87775, 1:200, Abcam) and SOX2 (PA1-094, 1:100, Thermo Fisher Scientific). Mouse antibodies were detected with goat anti-mouse-IgG antibody conjugated to Alexa Fluor 488, and rabbit antibodies were detected with goat anti-rabbit-IgG antibody conjugated to Alexa Fluor 568 (Thermo Fisher Scientific). All samples were counterstained with DAPI.

Nucleic acid extraction and gene expression

Total RNA was isolated from cells upon reaching 70–85% confluence with Trizol (Thermo Fisher Scientific) following the recommended protocol. Approximately 3.0 – 7.5×10^5 cells were used for all genomic DNA (gDNA) extractions with a DNeasy Blood & Tissue Kit (Qiagen, Hilden, Germany). Gene expression analysis was performed using TaqMan® gene expression assays (Thermo Fisher Scientific) for *APEX1* (Hs00959050_g1), *BRCAl* (Hs01556193_m1), *RPA1* (Hs00161419_m1), *RPA3* (Hs01047933_g1), *TET1* (Hs04189344_g1), *TET2* (Hs00325999_m1), *hTERT* (Hs00972656_m1), *POU5F1* (Hs00742896_s1), *SOX2* (Hs01053049_s1), *MYC* (Hs00153408_m1), *NANOG* (Hs04260366_g1), *KLF-4* (Hs00358836_m1), *LIN28A* (Hs00702808_s1), *DNMT1* (Hs00945875_m1), *DNMT3B* (Hs00171876_m1), *DNMT3A* (Hs01027162_m1) and *DNMT3L* (Hs01081364_m1). Endogenous housekeeping genes used were *ACTB* (Hs99999903_m1) and *PPIA* (Hs99999904_m1). All mRNA gene expression experiments were conducted using 50 ng of cDNA per experiment. MicroRNA was extracted using the TaqMan® microRNA Cells-to-C_T kit (Thermo Fisher Scientific). cDNA templates for miRNAs were created using the TaqMan® Advanced miRNA cDNA synthesis kit (Thermo Fisher Scientific) according to the manufacturer's protocol. TaqMan advanced miRNA assays (Thermo Fisher Scientific) used were miR-29a-3p (478587_mir), miR-29b-3p (478369_mir) and miR-29c-3p (479229_mir). The endogenous miRNA control was miR-361-5p (478056_mir). All quantitative RT-PCR experiments were conducted with a StepOnePlus Real-Time PCR System (Applied Biosystems). mRNA gene expression and miRNA expression analysis was conducted using the TaqMan® fast advanced master mix (Life Technologies). Graphical

representation of gene expression in HD-affected cells is relative to the mean expression of triplicate samples of two unaffected wild-type cell lines (as described in the cell lines and culture section). Relative fold-changes were calculated using the $2^{-\Delta\Delta Ct}$ method. Significance was determined using a one-way analysis of variance with a Dunnett's post hoc test. All experiments were independently conducted in triplicate.

Immunofluorescence imaging and quantitation

All immunofluorescence of cells was conducted on Lab-Tek microscope chamber slides at densities of 1.5×10^3 – 5.0×10^3 cells/cm². All NSC were plated onto Geltrex-coated slides and allowed to attach for 48–72 h. Cells were fixed with 10% NBF for 1 h, permeabilized with 100% ice-cold methanol for 15 min at -20°C , and blocked with 10% goat serum in Tris-buffered saline at room temperature for 1 h. To confirm successful NSC differentiation, cells were probed with antibodies for nestin (10C2, 1:100, Thermo Fisher Scientific), PAX6 (13B10-1A10, 1:200, Thermo Fisher Scientific), SOX1 (ab87775, 1:200, ABCAM, Cambridge, MA) and SOX2 (PA1-094, 1:100, Thermo Fisher Scientific). Primary antibodies for TET expression were against TET1 (GT1462, 1:500, Thermo Fisher Scientific) and TET2 (ab94580, 10 $\mu\text{g}/\text{ml}$, Abcam). Mouse antibodies were detected with goat anti-mouse-IgG conjugated to Alexa Fluor 488 (1:1000), and rabbit antibodies were detected with goat anti-rabbit-IgG conjugated to Alexa Fluor 568 (1:1000) (Thermo Fisher Scientific) for 1 h at room temperature. All samples were counterstained with DAPI. Fluorescent images were acquired with a Zeiss Axio Observer.Z1 microscope (Carl Zeiss AG, Jena, Germany) with either 10 \times or 20 \times objectives. ImageJ software version 1.51p FIJI (National Institutes of Health, Bethesda, MD; <http://imagej.nih.gov/ij>) was used to determine fluorescence quantitation. At least five images from each slide sample were acquired for relative quantitation measurements. Cell fluorescence was determined by multiplying the total area of the image by mean background of the image, which was then subtracted from the integrated density. The cell fluorescence of each image was divided by the number of complete nuclei within the image to acquire the corrected total cell fluorescence (CTCF). Mean CTCF is represented graphically as relative values normalized to the mean for the Wt cells. Statistical analysis was conducted using the Wilcoxon rank sum test of the relative fold changes.

Western blot analysis

For protein extraction, passage-matched unaffected Wt and HD-affected NSCs were homogenized in RIPA buffer supplemented with protease inhibitor cocktail (10 $\mu\text{g}/\text{ml}$, Sigma Aldrich). The sample was then centrifuged at 12,000 g and the supernatant was collected for analysis. Protein extracts were quantified using a bicinchoninic acid kit (Thermo Fisher Scientific). Samples were diluted accordingly in RIPA buffer to achieve similar concentrations. A total of 20 μg of protein was mixed with Laemmli loading buffer and electrophoresed on a 7.5% Tris/glycine/SDS polyacrylamide gel at 150 V for 45 min. Samples were transferred onto polyvinylidene fluoride membranes (Bio-Rad). Membranes were probed with primary antibodies against TET1 (GT1462, 1:1000, Thermo Fisher Scientific), TET2 (P411, 1:1500, Thermo Fisher Scientific) and ACTB (ab8224, 1 $\mu\text{g}/\text{ml}$, ABCAM) overnight at 4°C and resolved using the VECTASTAIN ABC-AmP kit (Vector Laboratories, Burlingame, CA) according to the manufacturer's protocol. Immunoreactive protein bands were imaged using a myECL Imager (Thermo Fisher Scientific) and quantified by optical densitometry using ImageJ software (NIH). Protein quantities were normalized to ACTB. Data is expressed as the mean \pm s.d. Statistical analysis was conducted with a one-way ANOVA with a post hoc Tukey's test between groups using GraphPad Prism 7.03.

TET knockdown using siRNA

To evaluate the direct link between TET expression and expression of select DNA repair genes, 2.5×10^4 cells from early passage NSCs were plated onto a 12-well plate. Upon reaching 40–60% confluency, 6 pmol of Silencer Select Pre-designed siRNA (Thermo Fisher Scientific) for TET1 (Ambion; ID: n368212) or TET2 siRNA (Ambion; ID: s29441) or scrambled (Ambion; ID: 4390843) was introduced into cultures using Lipofectamine[®]

RNAiMAX Transfection Reagent (Thermo Fisher Scientific) according to the manufacturer's protocol. All experimental variations were completed with $n=4$. After 72 h, cells were harvested, and RNA was extracted and purified and transcribed into cDNA as described above. Statistical analysis was conducted with a one-way ANOVA with a post hoc Tukey's test between groups using GraphPad Prism 7.03.

Fragment analysis and triplet-repeat primed PCR

Determination of *HTT* gene expansion was conducted using triplet-repeat primed PCR in conjunction with capillary electrophoresis fragment analysis (Mollica et al., 2016). Briefly, in-house designed primers were synthesized by Integrated DNA Technologies (Coralville, IA). The forward primer was 5'-ATGAAGGCCTTCGAGTCCCTCAAGTC-3' with a carboxyfluorescein at its 5' end, and the reverse primer was 5'-CGGTGGCGGCTGTTGCTGCTGCTGCTGCTG-3' (Jama et al., 2013). The repetitive (CTG) sequence at the 3' end of the reverse primer allowed for non-specific binding of the primer, while the 5' end specificity ensures complete amplification of only the gene-specific sequence. Amplification of 50 ng of gDNA was conducted using Platinum[™] Taq DNA Polymerase High Fidelity (Invitrogen). A complete PCR consisted of 1 \times high-fidelity PCR buffer, 2.0 mM MgSO₄, 2.0 mM betaine (Sigma Aldrich), 0.2 mM dNTP mix, 0.2 μM of each primer, 1 U Platinum[®] Taq DNA Polymerase, with sterile water up to 25 μl . PCR conditions were as follows: 94.0°C for a 1-min initial denaturation, followed by 35 cycles of 94.0°C for 1 min, 64.0°C for 1 min, 72.0°C for 2 min, and a final extension at 72.0°C for 15 min. A 1 μl sample of each reaction was combined with 9.0 μl of Hi-Di formamide (Life Technologies) and 1.0 μl of Mapmarker 1000 X-Rhodamine-labeled internal size standard (BioVentures Inc., Murfreesboro, TN) in a thin-walled 0.2 ml PCR tube. Samples were heated to 95.0°C for 2 min to denature the amplicons, and then immediately placed onto ice for 10 min. Capillary electrophoresis was conducted on an Applied Biosystems 3130 Genetic Analyzer with 50-cm arrays and POP-6 Polymer (Applied Biosystems). Electrokinetic injection of samples was initiated with 1.6 kV for 15 s, and then resolved at 15 kV for 2000 s at 60.0°C . Raw data were analyzed using GeneMarker software version 2.6.7 (SoftGenetics LLC, State College, PA) (Jama et al., 2013). Macros for sample binning were customized using six HD-affected and unaffected, homozygous and heterozygous gDNA samples obtained from Coriell Cell Repositories.

5-hydroxymethylcytosine detection

Relative levels of 5-hmC was detected in passage-identical cell types from unaffected Wt cell lines and HD-affected cell lines. Global detection was completed using the Quest 5-hmC[™] DNA ELISA kit (Zymo Research, Irvine, CA; D5426) according to the supplied protocol. Diluted anti-5-hydroxymethylcytosine polyclonal antibody (1 ng/ μl) was used to coat the plate and allowed to incubate at 37°C for 1 h. After incubation, each well was washed twice with 1 \times ELISA buffer, and then allowed to remain for 30 min. gDNA was diluted to 50 ng/ μl in 1 \times ELISA buffer, denatured at 98.0°C for 5 min, and then immediately placed onto ice for 10 min. DNA was further diluted to 1 ng/ μl in buffer. A total of 100 μl of dilute gDNA was placed into wells and incubated at 37°C for 1 h. Following incubation and successive washes, anti-DNA horseradish peroxidase-conjugated antibody (Zymo Research, Irvine, CA; A4001-25, 1:100) was added for 30 min. Each well was then washed four times, and developer was added at room temperature for 30 min. Absorbance at 405 nm was detected using a SpectraMax i3 Multi-Mode Detection System microplate reader (Molecular Devices, Sunnyvale, CA). Each sample was run in quadruplicate. Data represented is the mean \pm s.d. percentage (%) 5-hmC, relative to five sets of control DNA supplied with the assay. Statistical analysis was conducted with a one-way ANOVA with a post hoc Tukey's test between groups using GraphPad Prism 7.03.

Acknowledgements

We would like to acknowledge the services of Mrs Mary Ann Clements and Mr Michael K. Gubler from the Eastern Virginia Medical School Histology Services Laboratory.

Competing interests

The authors declare no competing or financial interests.

Author contributions

Conceptualization: R.D.B., P.C.S.; Methodology: P.A.M., J.A.R., R.D.B., P.C.S.; Formal analysis: P.A.M., M.Z., R.D.B., P.C.S.; Investigation: P.A.M., M.Z., J.A.R., D.K.S., A.E.W.; Resources: R.D.B., P.C.S.; Writing - original draft: P.A.M., R.D.B., P.C.S.; Writing - review & editing: P.A.M., R.D.B., P.C.S.; Visualization: P.A.M., M.Z., R.D.B., P.C.S.; Supervision: R.C.O., R.D.B., P.C.S.; Project administration: R.D.B., P.C.S.; Funding acquisition: R.D.B., P.C.S.

Funding

This research received no specific grant from any funding agency in the public, commercial or not-for-profit sectors. Funding for this work was provided through institutional start-up funds to P.C.S. and R.D.B. furnished through the Old Dominion University College of Health Sciences.

Supplementary information

Supplementary information available online at <http://jcs.biologists.org/lookup/doi/10.1242/jcs.215343.supplemental>

References

- Al-Mahdawi, S., Virmouni, S. A. and Pook, M. A. (2014). The emerging role of 5-hydroxymethylcytosine in neurodegenerative diseases. *Front. Neurosci.* **8**, 397.
- Andreoni, F., Darmon, E., Poon, W. C. and Leach, D. R. (2010). Overexpression of the single-stranded DNA-binding protein (SSB) stabilises CAG*CTG triplet repeats in an orientation dependent manner. *FEBS Lett.* **584**, 153-158.
- Beaver, J. M., Lai, Y., Xu, M., Casin, A. H., Laverde, E. E. and Liu, Y. (2015). AP endonuclease 1 prevents trinucleotide repeat expansion via a novel mechanism during base excision repair. *Nucleic Acids Res.* **43**, 5948-5960.
- Boulanger, C. A., Bruno, R. D., Mack, D. L., Gonzales, M., Castro, N. P., Salomon, D. S. and Smith, G. H. (2013). Embryonic stem cells are redirected to non-tumorigenic epithelial cell fate by interaction with the mammary microenvironment. *PLoS ONE* **8**, e62019.
- Boulanger, C. A., Bruno, R. D., Rosu-Myles, M. and Smith, G. H. (2012). The mouse mammary microenvironment redirects mesoderm-derived bone marrow cells to a mammary epithelial progenitor cell fate. *Stem Cells Dev.* **21**, 948-954.
- Broderick, S., Rehmet, K., Concannon, C. and Nasheuer, H. P. (2010). Eukaryotic single-stranded DNA binding proteins: central factors in genome stability. *Subcell. Biochem.* **50**, 143-163.
- Bruno, R. D., Boulanger, C. A., Rosenfield, S. M., Anderson, L. H., Lydon, J. P. and Smith, G. H. (2014). Paracrine-rescued lobulogenesis in chimeric outgrowths comprising progesterone-receptor-null mammary epithelium and redirected wild-type testicular cells. *J. Cell Sci.* **127**, 27-32.
- Bruno, R. D., Fleming, J. M., George, A. L., Boulanger, C. A., Schedin, P. and Smith, G. H. (2017). Mammary extracellular matrix directs differentiation of testicular and embryonic stem cells to form functional mammary glands in vivo. *Sci. Rep.* **7**, 40196.
- Brustovetsky, N. (2015). Mutant huntingtin and elusive defects in oxidative metabolism and mitochondrial calcium handling. *Mol. Neurobiol.* **53**, 2944-2953.
- Buckley, N. J., Johnson, R., Zuccato, C., Bithell, A. and Cattaneo, E. (2010). The role of REST in transcriptional and epigenetic dysregulation in Huntington's disease. *Neurobiol. Dis.* **39**, 28-39.
- Bussard, K. M., Boulanger, C. A., Booth, B. W., Bruno, R. D. and Smith, G. H. (2010). Reprogramming human cancer cells in the mouse mammary gland. *Cancer Res.* **70**, 6336-6343.
- Carey, B. W., Markoulaki, S., Hanna, J. H., Faddah, D. A., Buganim, Y., Kim, J., Ganz, K., Steine, E. J., Cassidy, J. P., Creighton, M. P. et al. (2011). Reprogramming factor stoichiometry influences the epigenetic state and biological properties of induced pluripotent stem cells. *Cell Stem Cell* **9**, 588-598.
- Chae, J. I., Kim, D. W., Lee, N., Jeon, Y. J., Jeon, I., Kwon, J., Kim, J., Soh, Y., Lee, D. S., Seo, K. S. et al. (2012). Quantitative proteomic analysis of induced pluripotent stem cells derived from a human Huntington's disease patient. *Biochem. J.* **446**, 359-371.
- Chang, K. H., Chen, Y. C., Wu, Y. R., Lee, W. F. and Chen, C. M. (2012). Downregulation of genes involved in metabolism and oxidative stress in the peripheral leukocytes of Huntington's disease patients. *PLoS ONE* **7**, e46492.
- Choi, S. H., Kim, Y. H., Hebisch, M., Sliwinski, C., Lee, S., D'Avanzo, C., Chen, H., Hooli, B., Asselin, C., Muffat, J. et al. (2014). A three-dimensional human neural cell culture model of Alzheimer's disease. *Nature* **515**, 274-278.
- Crespan, E., Hübscher, U. and Maga, G. (2015). Expansion of CAG triplet repeats by human DNA polymerases lambda and beta in vitro, is regulated by flap endonuclease 1 and DNA ligase 1. *DNA Repair (Amst)* **29**, 101-111.
- Dawlaty, M. M., Breiling, A., Le, T., Barrasa, M. I., Raddatz, G., Gao, Q., Powell, B. E., Cheng, A. W., Faull, K. F., Lyko, F. et al. (2014). Loss of Tet enzymes compromises proper differentiation of embryonic stem cells. *Dev. Cell* **29**, 102-111.
- del Hoyo, P., Garcia-Redondo, A., de Bustos, F., Molina, J. A., Sayed, Y., Alonso-Navarro, H., Caballero, L., Arenas, J. and Jimenez-Jimenez, F. J. (2006). Oxidative stress in skin fibroblasts cultures of patients with Huntington's disease. *Neurochem. Res.* **31**, 1103-1109.
- Dion, V. (2014). Tissue specificity in DNA repair: lessons from trinucleotide repeat instability. *Trends Genet.* **30**, 220-229.
- Dragileva, E., Hendricks, A., Teed, A., Gillis, T., Lopez, E. T., Friedberg, E. C., Kucherlapati, R., Edelman, W., Lunetta, K. L., MacDonald, M. E. et al. (2009). Intergenerational and striatal CAG repeat instability in Huntington's disease knock-in mice involve different DNA repair genes. *Neurobiol. Dis.* **33**, 37-47.
- Dunah, A. W., Jeong, H., Griffin, A., Kim, Y. M., Standaert, D. G., Hersch, S. M., Mouradian, M. M., Young, A. B., Tanese, N. and Krainc, D. (2002). Sp1 and TAFII130 transcriptional activity disrupted in early Huntington's disease. *Science* **296**, 2238-2243.
- Fortune, M. T., Vassilopoulos, C., Coolbaugh, M. I., Siciliano, M. J. and Monkton, D. G. (2000). Dramatic, expansion-biased, age-dependent, tissue-specific somatic mosaicism in a transgenic mouse model of triplet repeat instability. *Hum. Mol. Genet.* **9**, 439-445.
- Glajch, K. E. and Sadri-Vakili, G. (2015). Epigenetic mechanisms involved in Huntington's disease pathogenesis. *J. Huntingtons Dis.* **4**, 1-15.
- Goula, A.-V., Berquist, B. R., Wilson, D. M., III, Wheeler, V. C., Trotter, Y. and Merienne, K. (2009). Stoichiometry of base excision repair proteins correlates with increased somatic CAG instability in striatum over cerebellum in Huntington's disease transgenic mice. *PLoS Genet.* **5**, e1000749.
- Goula, A.-V. and Merienne, K. (2013). Abnormal base excision repair at trinucleotide repeats associated with diseases: a tissue-selective mechanism. *Genes (Basel)* **4**, 375-387.
- HD iPSC Consortium (2012). Induced pluripotent stem cells from patients with Huntington's disease show CAG-repeat-expansion-associated phenotypes. *Cell Stem Cell* **11**, 264-278.
- Hewitt, K. J., Shamis, Y., Hayman, R. B., Margvelashvili, M., Dong, S., Carlson, M. W. and Garlick, J. A. (2011). Epigenetic and phenotypic profile of fibroblasts derived from induced pluripotent stem cells. *PLoS ONE* **6**, e17128.
- Hick, A., Wattenhofer-Donze, M., Chintawar, S., Tropel, P., Simard, J. P., Vaucamps, N., Gall, D., Lambot, L., Andre, C., Reutenauer, L. et al. (2013). Neurons and cardiomyocytes derived from induced pluripotent stem cells as a model for mitochondrial defects in Friedreich's ataxia. *Dis. Model Mech.* **6**, 608-621.
- Hysolli, E., Tanaka, Y., Su, J., Kim, K.-Y., Zhong, T., Janknecht, R., Zhou, X.-L., Geng, L., Qiu, C., Pan, X. et al. (2016). Regulation of the DNA Methylation Landscape in Human Somatic Cell Reprogramming by the miR-29 Family. *Stem Cell Reports* **7**, 43-54.
- Ito, S., D'Alessio, A. C., Taranova, O. V., Hong, K., Sowers, L. C. and Zhang, Y. (2010). Role of Tet proteins in 5mC to 5hmC conversion, ES-cell self-renewal and inner cell mass specification. *Nature* **466**, 1129-1133.
- Jama, M., Millson, A., Miller, C. E. and Lyon, E. (2013). Triplet repeat primed PCR simplifies testing for Huntington disease. *J. Mol. Diagn.* **15**, 255-262.
- Jeon, I., Choi, C., Lee, N., Im, W., Kim, M., Oh, S.-H., Park, I.-H., Kim, H. S. and Song, J. (2014). In vivo roles of a patient-derived induced pluripotent stem cell line (HD72-iPSC) in the YAC128 model of Huntington's disease. *Int. J. Stem Cells* **7**, 43-47.
- Jeon, I., Lee, N., Li, J.-Y., Park, I.-H., Park, K. S., Moon, J., Shim, S. H., Choi, C., Chang, D.-J., Kwon, J. et al. (2012). Neuronal properties, in vivo effects, and pathology of a Huntington's disease patient-derived induced pluripotent stem cells. *Stem Cells* **30**, 2054-2062.
- Johnson, R., Zuccato, C., Belyaev, N. D., Guest, D. J., Cattaneo, E. and Buckley, N. J. (2008). A microRNA-based gene dysregulation pathway in Huntington's disease. *Neurobiol. Dis.* **29**, 438-445.
- Jonson, I., Ougland, R. and Larsen, E. (2013). DNA repair mechanisms in Huntington's disease. *Mol. Neurobiol.* **47**, 1093-1102.
- Juopperi, T. A., Kim, W. R., Chiang, C.-H., Yu, H., Margolis, R. L., Ross, C. A., Ming, G.-L. and Song, H. (2012). Astrocytes generated from patient induced pluripotent stem cells recapitulate features of Huntington's disease patient cells. *Mol. Brain* **5**, 17.
- Kaye, J. A. and Finkbeiner, S. (2013). Modeling Huntington's disease with induced pluripotent stem cells. *Mol. Cell. Neurosci.* **56**, 50-64.
- Kinney, S. R. M. and Pradhan, S. (2013). Ten eleven translocation enzymes and 5-hydroxymethylation in mammalian development and cancer. *Adv. Exp. Med. Biol.* **754**, 57-79.
- Koh, K. P., Yabuuchi, A., Rao, S., Huang, Y., Cunniff, K., Nardone, J., Laiho, A., Tahiliani, M., Sommer, C. A., Mostoslavsky, G. et al. (2011). Tet1 and Tet2 regulate 5-hydroxymethylcytosine production and cell lineage specification in mouse embryonic stem cells. *Cell Stem Cell* **8**, 200-213.
- Kovtun, I. V., Thornhill, A. R. and McMurray, C. T. (2004). Somatic deletion events occur during early embryonic development and modify the extent of CAG expansion in subsequent generations. *Hum. Mol. Genet.* **13**, 3057-3068.
- Kriaucionis, S. and Heintz, N. (2009). The nuclear DNA base 5-hydroxymethylcytosine is present in Purkinje neurons and the brain. *Science* **324**, 929-930.
- Langbehn, D. R., Brinkman, R. R., Falush, D., Paulsen, J. S. and Hayden, M. R. and International Huntington's Disease Collaborative Group. (2004). A new

- model for prediction of the age of onset and penetrance for Huntington's disease based on CAG length. *Clin. Genet.* **65**, 267-277.
- Langbehn, D. R., Hayden, M. R. and Paulsen, J. S. and PREDICT-HD Investigators of the Huntington Study Group (2010). CAG-repeat length and the age of onset in Huntington disease (HD): a review and validation study of statistical approaches. *Am. J. Med. Genet. B Neuropsychiatr. Genet.* **153B**, 397-408.
- Lee, J., Hwang, Y. J., Kim, K. Y., Kowall, N. W. and Ryu, H. (2013). Epigenetic mechanisms of neurodegeneration in Huntington's disease. *Neurotherapeutics* **10**, 664-676.
- Lee, S. and Huang, E. J. (2017). Modeling ALS and FTD with iPSC-derived neurons. *Brain Res.* **1656**, 88-97.
- Leung, K. S., Cheng, V. W., Mok, S. W. and Tsui, S. K. (2014). The involvement of DNA methylation and histone modification on the epigenetic regulation of embryonic stem cells and induced pluripotent stem cells. *Curr. Stem Cell Res. Ther.* **9**, 388-395.
- Li, M., Völker, J., Breslauer, K. J. and Wilson, D. M.III. (2014). APE1 incision activity at abasic sites in tandem repeat sequences. *J. Mol. Biol.* **426**, 2183-2198.
- Liu, Y. and Wilson, S. H. (2012). DNA base excision repair: a mechanism of trinucleotide repeat expansion. *Trends Biochem. Sci.* **37**, 162-172.
- MacDonald, M. E., Ambrose, C. M., Duyao, M. P., Myers, R. H., Lin, C., Srinidhi, L., Barnes, G., Taylor, S. A., James, M., Groot, N. et al. (1993). A novel gene containing a trinucleotide repeat that is expanded and unstable on Huntington's disease chromosomes. The huntington's disease collaborative research group. *Cell* **72**, 971-983.
- Mangiarini, L., Sathasivam, K., Mahal, A., Mott, R., Seller, M. and Bates, G. P. (1997). Instability of highly expanded CAG repeats in mice transgenic for the Huntington's disease mutation. *Nat. Genet.* **15**, 197-200.
- Mann, V. M., Cooper, J. M., Javoy-Agid, F., Agid, Y., Jenner, P. and Schapira, A. H. (1990). Mitochondrial function and parental sex effect in Huntington's disease. *Lancet* **336**, 749.
- Martí, E., Pantano, L., Bañez-Coronel, M., Llorens, F., Miñones-Moyano, E., Porta, S., Sumoy, L., Ferrer, I. and Estivill, X. (2010). A myriad of miRNA variants in control and Huntington's disease brain regions detected by massively parallel sequencing. *Nucleic Acids Res.* **38**, 7219-7235.
- Mason, A. G., Tomé, S., Simard, J. P., Libby, R. T., Bammler, T. K., Beyer, R. P., Morton, A. J., Pearson, C. E. and La Spada, A. R. (2014). Expression levels of DNA replication and repair genes predict regional somatic repeat instability in the brain but are not altered by polyglutamine disease protein expression or age. *Hum. Mol. Genet.* **23**, 1606-1618.
- McQuade, L. R., Balachandran, A., Scott, H. A., Khaira, S., Baker, M. S. and Schmidt, U. (2014). Proteomics of Huntington's disease-affected human embryonic stem cells reveals an evolving pathology involving mitochondrial dysfunction and metabolic disturbances. *J. Proteome Res.* **13**, 5648-5659.
- Mollica, P. A., Reid, J. A., Ogle, R. C., Sachs, P. C. and Bruno, R. D. (2016). DNA methylation leads to DNA repair gene down-regulation and trinucleotide repeat expansion in patient-derived huntington disease cells. *Am. J. Pathol.* **186**, 1967-1976.
- Morita, S., Horii, T., Kimura, M., Ochiya, T., Tajima, S. and Hatada, I. (2013). miR-29 represses the activities of DNA methyltransferases and DNA demethylases. *Int. J. Mol. Sci.* **14**, 14647-14658.
- Nayler, S. P., Powell, J. E., Vanichkina, D. P., Korn, O., Wells, C. A., Kanjhan, R., Sun, J., Taft, R. J., Lavin, M. F. and Wolvetang, E. J. (2017). Human iPSC-derived cerebellar neurons from a patient with ataxia-telangiectasia reveal disrupted gene regulatory networks. *Front. Cell Neurosci.* **11**, 321.
- Nenasheva, V. V., Novosadova, E. V., Makarova, I. V., Lebedeva, O. S., Grefenshtein, M. A., Arsenyeva, E. L., Antonov, S. A., Grivennikov, I. A. and Tarantul, V. Z. (2016). The transcriptional changes of trim genes associated with Parkinson's disease on a model of human induced pluripotent stem cells. *Mol. Neurobiol.* **54**, 7204-7211.
- Ng, C. W., Yildirim, F., Yap, Y. S., Dalin, S., Matthews, B. J., Velez, P. J., Labadorf, A., Housman, D. E. and Fraenkel, E. (2013). Extensive changes in DNA methylation are associated with expression of mutant huntingtin. *Proc. Natl. Acad. Sci. USA* **110**, 2354-2359.
- Nucifora, F. C., Jr, Sasaki, M., Peters, M. F., Huang, H., Cooper, J. K., Yamada, M., Takahashi, H., Tsuji, S., Troncoso, J., Dawson, V. L. et al. (2001). Interference by huntingtin and atrophin-1 with cbp-mediated transcription leading to cellular toxicity. *Science* **291**, 2423-2428.
- Pan, Y., Daito, T., Sasaki, Y., Chung, Y. H., Xing, X., Pondugula, S., Swamidass, S. J., Wang, T., Kim, A. H. and Yano, H. (2016). Inhibition of DNA methyltransferases blocks mutant huntingtin-induced neurotoxicity. *Sci. Rep.* **6**, 31022.
- Ranen, N. G., Stine, O. C., Abbott, M. H., Sherr, M., Codori, A. M., Franz, M. L., Chao, N. I., Chung, A. S., Pleasant, N., Callahan, C. et al. (1995). Anticipation and instability of IT-15 (CAG)_n repeats in parent-offspring pairs with Huntington disease. *Am. J. Hum. Genet.* **57**, 593-602.
- Roshan, R., Shridhar, S., Sarangdhar, M. A., Banik, A., Chawla, M., Garg, M., Singh, V. P. and Pillai, B. (2014). Brain-specific knockdown of miR-29 results in neuronal cell death and ataxia in mice. *RNA* **20**, 1287-1297.
- Rudenko, A., Dawlaty, M. M., Seo, J., Cheng, A. W., Meng, J., Le, T., Faull, K. F., Jaenisch, R. and Tsai, L.-H. (2013). Tet1 is critical for neuronal activity-regulated gene expression and memory extinction. *Neuron* **79**, 1109-1122.
- Sachs, P. C., Francis, M. P., Zhao, M., Brumelle, J., Rao, R. R., Elmore, L. W. and Holt, S. E. (2012). Defining essential stem cell characteristics in adipose-derived stromal cells extracted from distinct anatomical sites. *Cell Tissue Res.* **349**, 505-515.
- Santiago, M., Antunes, C., Guedes, M., Sousa, N. and Marques, C. J. (2014). TET enzymes and DNA hydroxymethylation in neural development and function - how critical are they? *Genomics* **104**, 334-340.
- Spiro, C. and McMurray, C. T. (2003). Nuclease-deficient FEN-1 blocks Rad51/BRCA1-mediated repair and causes trinucleotide repeat instability. *Mol. Cell. Biol.* **23**, 6063-6074.
- Suzuki, M. M. and Bird, A. (2008). DNA methylation landscapes: provocative insights from epigenomics. *Nat. Rev. Genet.* **9**, 465-476.
- Tsoi, H., Lau, T. C.-K., Tsang, S.-Y., Lau, K.-F. and Chan, H. Y. E. (2012). CAG expansion induces nucleolar stress in polyglutamine diseases. *Proc. Natl. Acad. Sci. USA* **109**, 13428-13433.
- Vaskova, E. A., Stekleneva, A. E., Medvedev, S. P. and Zakian, S. M. (2013). "Epigenetic memory" phenomenon in induced pluripotent stem cells. *Acta Naturae* **5**, 15-21.
- Wang, F., Yang, Y., Lin, X., Wang, J.-Q., Wu, Y.-S., Xie, W., Wang, D., Zhu, S., Liao, Y.-Q., Sun, Q. et al. (2013). Genome-wide loss of 5-hmC is a novel epigenetic feature of Huntington's disease. *Hum. Mol. Genet.* **22**, 3641-3653.
- Zhai, W., Jeong, H., Cui, L., Krainc, D. and Tjian, R. (2005). In vitro analysis of huntingtin-mediated transcriptional repression reveals multiple transcription factor targets. *Cell* **123**, 1241-1253.
- Zhang, P., Huang, B., Xu, X. and Sessa, W. C. (2013). Ten-eleven translocation (Tet) and thymine DNA glycosylase (TDG), components of the demethylation pathway, are direct targets of miRNA-29a. *Biochem. Biophys. Res. Commun.* **437**, 368-373.
- Zhao, X.-N. and Usdin, K. (2015). The repeat expansion diseases: the dark side of DNA repair. *DNA Repair (Amst)* **32**, 96-105.
- Zhao, M., Sachs, P. C., Wang, X., Dumur, C. I., Idowu, M. O., Robila, V., Francis, M. P., Ware, J., Beckman, M., Rizki, A. et al. (2012). Mesenchymal stem cells in mammary adipose tissue stimulate progression of breast cancer resembling the basal-type. *Cancer Biol. Ther.* **13**, 782-792.